

Self-Healable, Stretchable, Transparent Triboelectric Nanogenerators as Soft Power Sources

Jiangman Sun,^{†,‡} Xiong Pu,^{*,†,‡,§} Mengmeng Liu,^{†,‡} Aifang Yu,^{†,‡,§} Chunhua Du,^{†,‡} Junyi Zhai,^{†,‡,§} Weiguo Hu,^{*,†,‡,§} and Zhong Lin Wang^{*,†,‡,§,||}

[†]CAS Center for Excellence in Nanoscience, Beijing Key Laboratory of Micro-nano Energy and Sensor, Beijing Institute of Nanoenergy and Nanosystems, Chinese Academy of Sciences, Beijing 100083, China

[‡]School of Nanoscience and Technology, University of Chinese Academy of Sciences, Beijing 100049, China

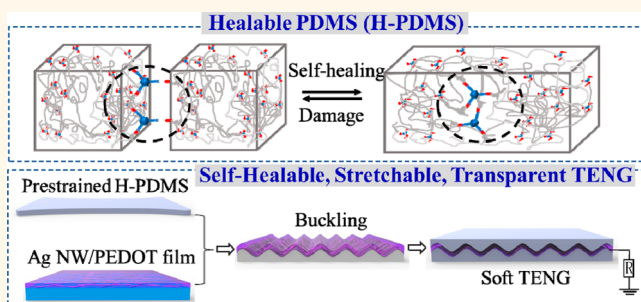
[§]Center on Nanoenergy Research, School of Physical Science and Technology, Guangxi University, Nanning 530004, China

^{||}School of Materials Science and Engineering, Georgia Institute of Technology, Atlanta, Georgia 30332-0245, United States

Supporting Information

ABSTRACT: Despite the rapid advancements of soft electronics, developing compatible energy devices will be the next challenge for their viable applications. Here, we report an energy-harnessing triboelectric nanogenerator (TENG) as a soft electrical power source, which is simultaneously self-healable, stretchable, and transparent. The nanogenerator features a thin-film configuration with buckled Ag nanowires/poly(3,4-ethylenedioxythiophene) composite electrode sandwiched in room-temperature self-healable poly(dimethylsiloxane) (PDMS) elastomers. Dynamic imine bonds are introduced in PDMS networks for repairing mechanical damages (94% efficiency), while the mechanical recovery of the elastomer is imparted to the buckled electrode for electrical healing. By adjusting the buckling wavelength of the electrode, the stretchability and transparency of the soft TENG can be tuned. A TENG (~50% stretchability, ~73% transmittance) can recover the electricity generation (100% healing efficiency) even after accidental cutting. Finally, the conversion of biomechanical energies into electricity (~100 V, 327 mW/m²) is demonstrated by a skin-like soft TENG. Considering all these merits, this work suggests a potentially promising approach for next-generation soft power sources.

KEYWORDS: self-healable, stretchable, transparent, triboelectric nanogenerator, energy skin



Next-generation electronics will be elastomeric, soft, and biocompatible.¹ For example, the booming epidermal electronics² or electronic skins,³ integrated with multiple sensing^{4,5} and medical cure capabilities,^{6,7} are reported to be flexible, stretchable, or even self-healable.^{8,9} Nevertheless, one subsequent challenge is to provide accordingly soft power sources to drive these devices.¹⁰ Motivated by this demand, extensive efforts have been made to develop soft/flexible, transparent, or self-healable energy-harvesting and storage devices.^{11–13} The triboelectric nanogenerator (TENG), based on the effects of triboelectrification and electrostatic induction, has been proven to be an efficient alternative to convert ubiquitous ambient mechanical energies into electricity, especially for mechanical motions at low frequencies.^{14,15} Previous works have demonstrated the viable applications of TENGs in powering various small electronics or in fabricating self-powered sensors/electronics.^{16–23} Furthermore, TENGs are naturally flexible due to their simple

structures and the use of dielectric polymers as electrification layers, making them highly promising for soft power sources.^{4,24,25} Transparent^{26–28} or highly stretchable^{29,30} TENGs have been therefore reported. By hybridizing elastomers and ionic conductive hydrogels, we previously reported a soft TENG that achieved simultaneously high transparency and stretchability.³¹ Nevertheless, due to the intrinsic energy-conversion mechanisms and materials/structure requirements, it is hard for TENGs and most other energy devices to realize transparency, stretchability, and self-healing ability simultaneously.^{12,32}

During the operation of TENGs, they are constantly exposed to external mechanical inputs (bending, twisting, pressing,

Received: April 3, 2018

Accepted: May 31, 2018

Published: May 31, 2018

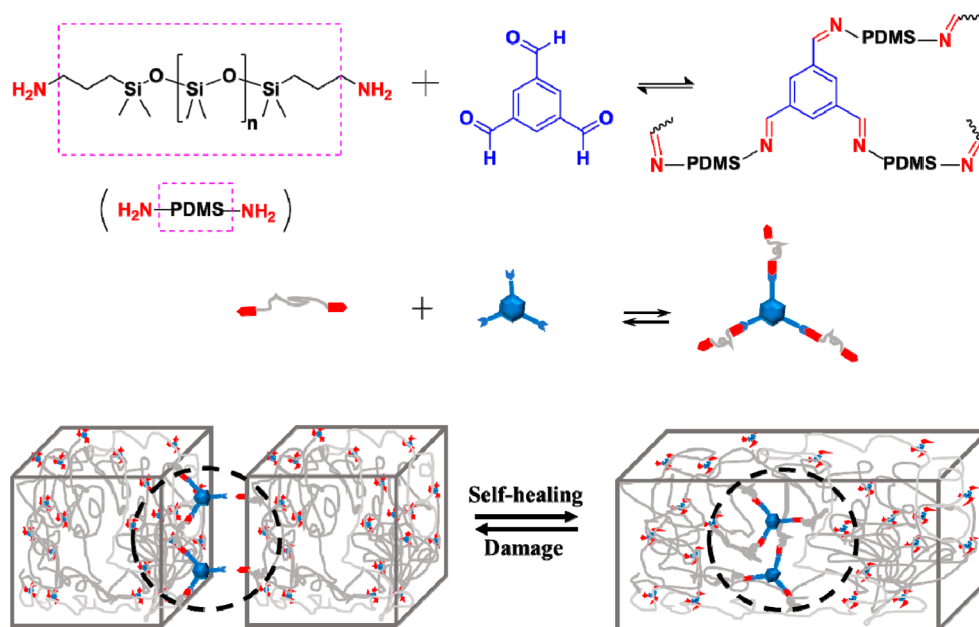


Figure 1. Self-healing mechanism of healable PDMS (H-PDMS). Bis(amine)-terminated PDMS and 1,3,5-triformylbenzene form reversible imine bonds through a Schiff base reaction, which are cleaved upon damage and recovered after an autonomous healing process.

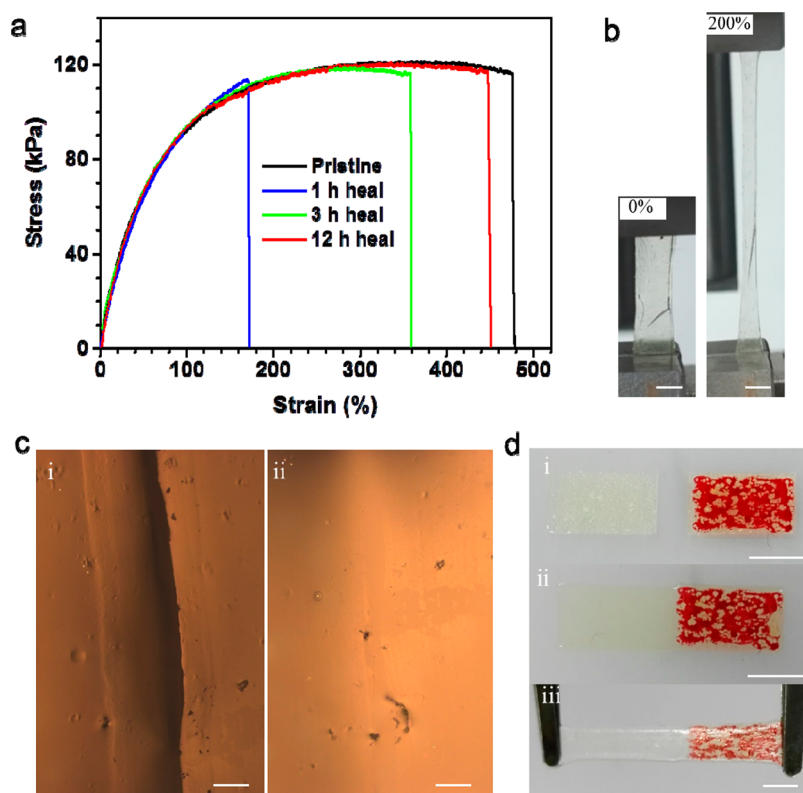


Figure 2. Self-healing properties of the H-PDMS. (a) The uniaxial tensile stress–strain profiles of pristine H-PDMS and H-PDMS healed for different periods of time at ambient conditions (21 °C) after cutting by a razor blade. (b) Optical photos of an H-PDMS in a stretched state. (c) Optical microscopy images of a cut H-PDMS (i) before and (ii) after 12 h of healing. (d) Optical photos showing an H-PDMS being (i) cut, (ii) 12 h healed, and (iii) stretched. Scale bar: 2 cm (b), 100 μm (c), and 1 cm (d).

sliding, *etc.*), which may cause mechanical damage and lead to malfunction. Meanwhile, accidental cutting or scratching is possible for soft power devices. Hence, an artificial self-healing capability, inspired by the inherent attribute of living organisms, is desirable for soft TENGs, so that damage can be repaired and functions can be recovered spontaneously.³³ A few efforts have

been made to explore healable TENGs.^{34–37} Shape-memory polymer polyurethane was applied as the electrification layer, micropatterns of which can be recovered upon heat treatment, but the whole device was not healable.³⁴ A self-healable ionic conductor was reported in a stretchable/transparent TENG, but the used electrification elastomers (silicone rubber and

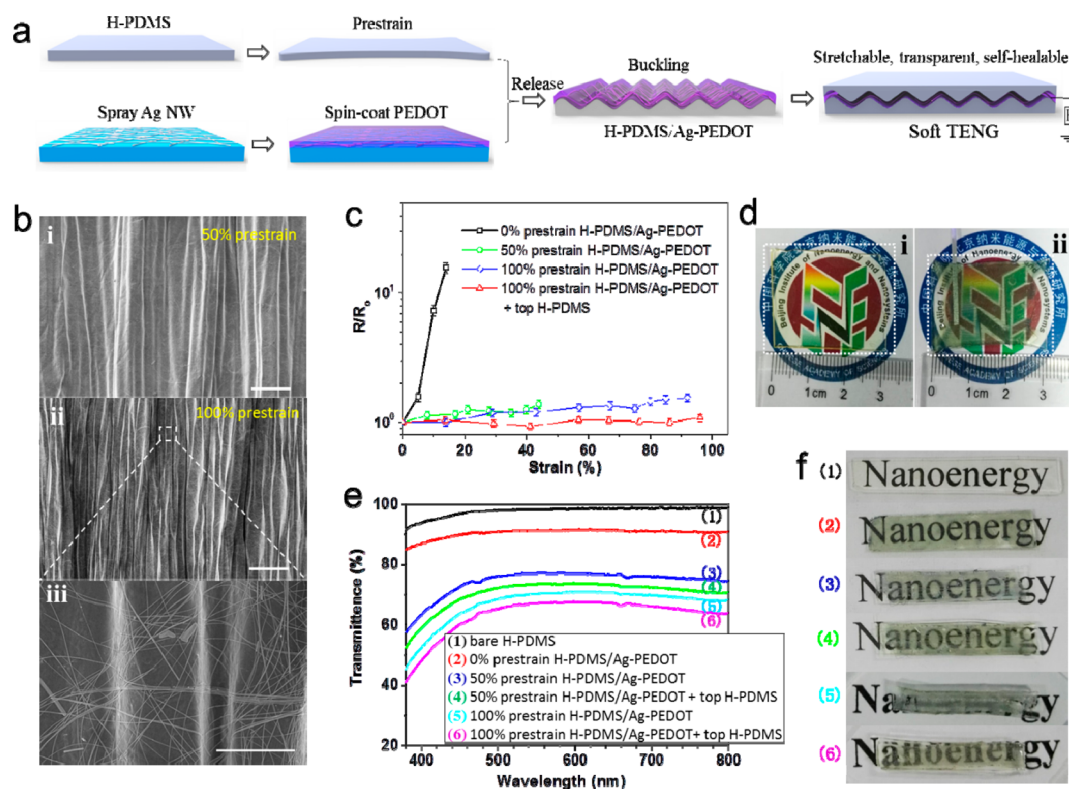


Figure 3. Fabrication and optimization of a self-healable, stretchable, and transparent TENG. (a) Schematic illustration of fabrication procedures of the Ag-PEDOT electrode by a prestrain–release–buckling process and the soft TENG by sealing an extra layer of H-PDMS. (b) SEM images of buckled Ag-PEDOT films with different amounts of prestrain, (i) 50% and (ii, iii) 100%. (c) Resistance variation of different Ag-PEDOT electrodes upon uniaxial stretching. (d) Optical photos of (i) a transparent bare H-PDMS film and (ii) an as-made soft TENG with 50% prestrain. (e) Ultraviolet–visible (UV–vis) spectra and (f) optical photos of a bare H-PDMS film, a H-PDMS/Ag-PEDOT film without prestrain, and prestrained H-PDMS/Ag-PEDOT films with or without a top H-PDMS layer. The labeling numbers in (f) are in accordance with that in (e). Scale bar: 50 μm (i, ii) and 5 μm (iii) of (b). The logo photos in (d) are used with permission from Beijing Institute of Nanoenergy and Nanosystems.

VHB tape) are not healable.³⁵ A fully healable TENG was reported by using the self-healing polymer polydimethylsiloxane–polyurethane, but heating was also needed, and the use of a magnetic electrode made the device rigid and unstretchable.³⁶ Therefore, further efforts are still required for developing room-temperature autonomously healable TENGs.

Here, we report a soft energy-harvesting TENG that is fully self-healable at ambient condition, stretchable, and transparent. The single-electrode mode TENG features a thin-film configuration with a buckled conductive thin electrode sandwiched between two healable elastomer films. The autonomously healable elastomer was prepared by introducing reversible dynamic imine bonds in the polymer networks of poly(dimethylsiloxane) (PDMS). The healable PDMS (H-PDMS) achieved 94% healing efficiency after curing at ambient conditions (21 °C for 12 h). The stretchable and transparent electrode was a composite film composed of Ag nanowires and poly(3,4-ethylenedioxythiophene) (Ag-PEDOT), which was transferred to the H-PDMS through a prestrain–release–buckling process. Although the electrode was not intrinsically healable, the healing of the H-PDMS can bring the damaged Ag-PEDOT film back into contact to restore the electrical conductivity. Therefore, the resulting TENG was stretchable, transparent, and able to recover its energy-generation function even after accidental cutting ($\sim 100\%$ healing efficiency). The TENG was demonstrated to scavenge mechanical motion energies of human bodies, outputting an open-circuit voltage of

~ 100 V and maximum power density of 327 mW/m^2 . This work provides a feasible approach for multifunctional soft power sources, which are potentially viable for the next-generation soft electronics.

RESULTS AND DISCUSSION

To achieve a healable TENG, the electrification polymer should be first mechanically healable. Recently, an intensive endeavor has been devoted to realizing an artificial healing ability through the strategies of microencapsulated healing agents,³⁸ dynamic noncovalent supermolecular assembly (hydrogen bonding,³⁹ metal–ligand coordination,⁴⁰ *etc.*), or reversible covalent bonding (Diels–Alder reaction,⁴¹ S–S bonds,⁴² imine,^{43,44} *etc.*).¹² Nevertheless, most of the reported healable polymers are not transparent or require external stimuli (heat, moisture, light, *etc.*) to trigger the healing process. In this work, we achieved an autonomously healable polymer that is stretchable and transparent as well. Dynamic covalent imine bonds were introduced into the PDMS networks as reversible healing sites. As shown in Figure 1, bis(amine)-terminated PDMS ($\text{H}_2\text{N-PDMS-NH}_2$) ($M_n = 5000\text{--}7000$ g mol^{-1}) reacts with 1,3,5-triformylbenzene (molar ratio is about 1:1) by a Schiff base reaction. The resulting reversible imine bonds function as both polymer cross-linker and self-healing points. Upon damage, imine bonds are cleaved and hydrolyzed back to aldehyde and amine, which will then generate imine bonds again and cure the damage in the healing process.⁴⁵ As shown by the Fourier

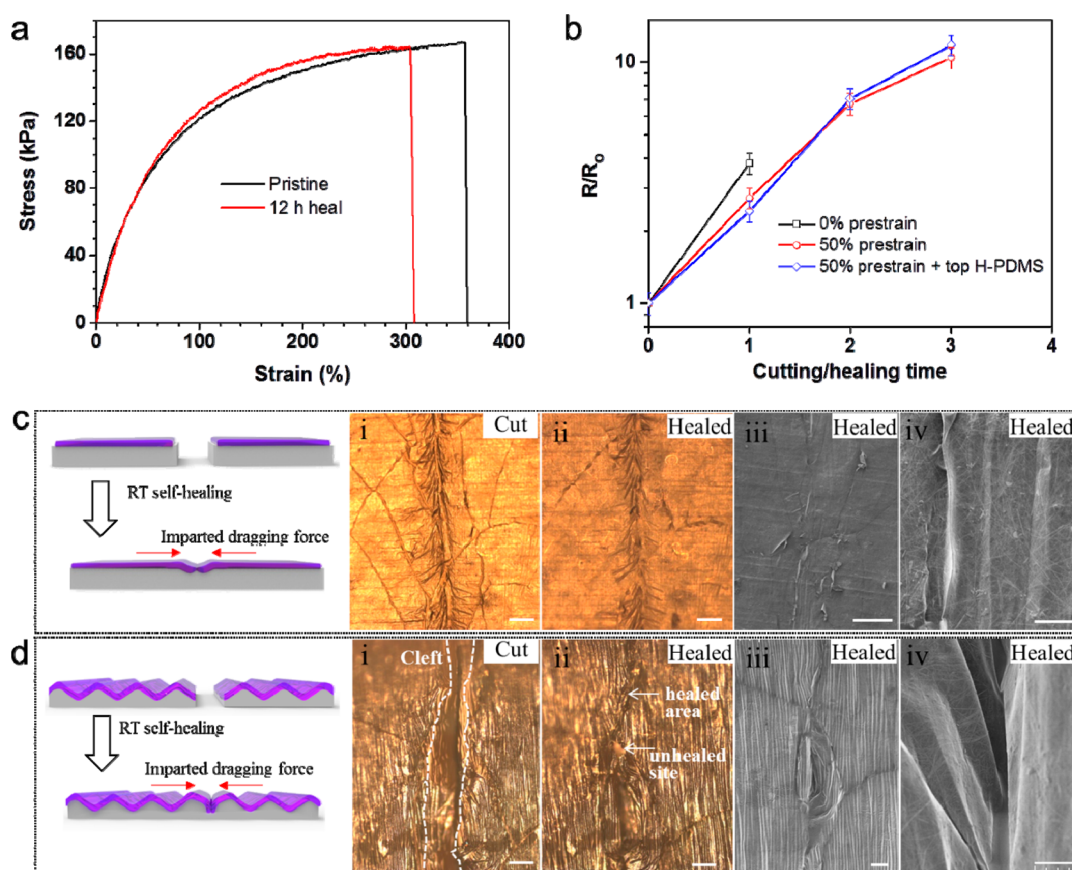


Figure 4. Mechanical and electrical self-healing properties of H-PDMS/Ag-PEDOT films. (a) Tensile stress–strain profiles of pristine and 12 h healed H-PDMS/Ag-PEDOT films. (b) Resistance variation ratios of different Ag-PEDOT films after multiple cutting and healing cycles. Schematic illustration and microscopy images of the (i) freshly cut and (ii–iv) 12 h healed (c) H-PDMS/Ag-PEDOT film without prestrain and (d) H-PDMS/Ag-PEDOT film with prestrain. Scale bar: 100 μm (i–iii) and 10 μm (iv).

transform infrared spectroscopy (FTIR) of the healable PDMS (H-PDMS) in Figure S1, peaks related to $-\text{C}=\text{O}-$ and $-\text{C}=\text{N}-$ stretching modes were observed at 1707 and 1648 cm^{-1} , respectively, confirming the excessive aldehyde groups and the formation of imine bonds in H-PDMS.

The as-fabricated H-PDMS is highly stretchable. At a uniaxial tensile speed of 40 mm min^{-1} , the ultimate strain to fracture is 476% at a stress of 116 kPa (Figure 2a). Optical images of the H-PDMS in the stretched state are shown in Figure 2b. The self-healing property was evaluated by tensile tests of H-PDMS which underwent an ambient healing process (21 $^{\circ}\text{C}$) for different periods of time (1, 3, and 12 h) after being cut completely with a razor blade. For all three samples, the ultimate stress recovers back to about $\sim 100\%$ of the pristine value; the healing efficiency calculated based on the strain to fracture is 36%, 75%, and 94% after 1, 3, and 12 h of healing, respectively (Figure 2a). Figure 2c shows that a $\sim 200 \mu\text{m}$ wide cleft was cured thoroughly after 12 h of ambient healing. For demonstration, an H-PDMS elastomer was cut into two pieces and attached back (Figure 2d). After 12 h of autonomous healing, the mechanical elasticity of the sample was fully recovered.

With the stretchable, transparent, and autonomously healable elastomer, the next challenge is to fabricate a conductive electrode with comparable properties. A prestrain–release–buckling process was adopted for synthesizing the electrode, as schematically illustrated in Figure 3a. This strategy, pioneered by Whitesides *et al.*, has been well studied recently to convert

inorganic or brittle materials into stretchable “wavy” conductors.⁴⁶ Here, a composite film of spray-coated Ag nanowire (NW) networks and spin-coated PEDOT film was selected as the electrical conductor, which was then transferred to a prestrained H-PDMS. By releasing the strain of the elastomeric substrate, the strongly adhered Ag-PEDOT film buckled spontaneously to form periodically wavy structures (Figure 3b). According to our experiences, the loosely stacked Ag NW film (Figure S2a) can hardly be attached onto the prestrained H-PDMS. Meanwhile, the polymer matrix may fuse into the Ag NW networks with time and block the conductive intercrossing contacts, leading to a reduced conductivity.⁴⁷ Hence, the PEDOT was spin-coated as an adhesive agent to anchor the networks for successful transfer (Figure S2b,c) and stable electrical properties. The sheet resistance of the pristine Ag-PEDOT film was measured to be about 11 Ω/square . Two samples with different prestrains were fabricated, *i.e.* $\sim 50\%$ (Figure 3b (i)) and $\sim 100\%$ (Figure 3b (ii)), respectively. The periodic wavy fringes can be observed to be perpendicular to the lateral prestrain direction. By increasing the prestrain, the buckling fringes become denser (*i.e.*, smaller buckling wavelength). Even with a prestrain of $\sim 100\%$, the buckled composite film was not damaged and the Ag NWs adhere to the substrate conformally without fracture (Figure 3b (iii)). Upon stretching, the wavy Ag-PEDOT film can accommodate the strain by increasing the buckling wavelength and decreasing the buckling amplitude, so the strain rendered on the Ag-PEDOT film itself is significantly reduced. As for a transferred

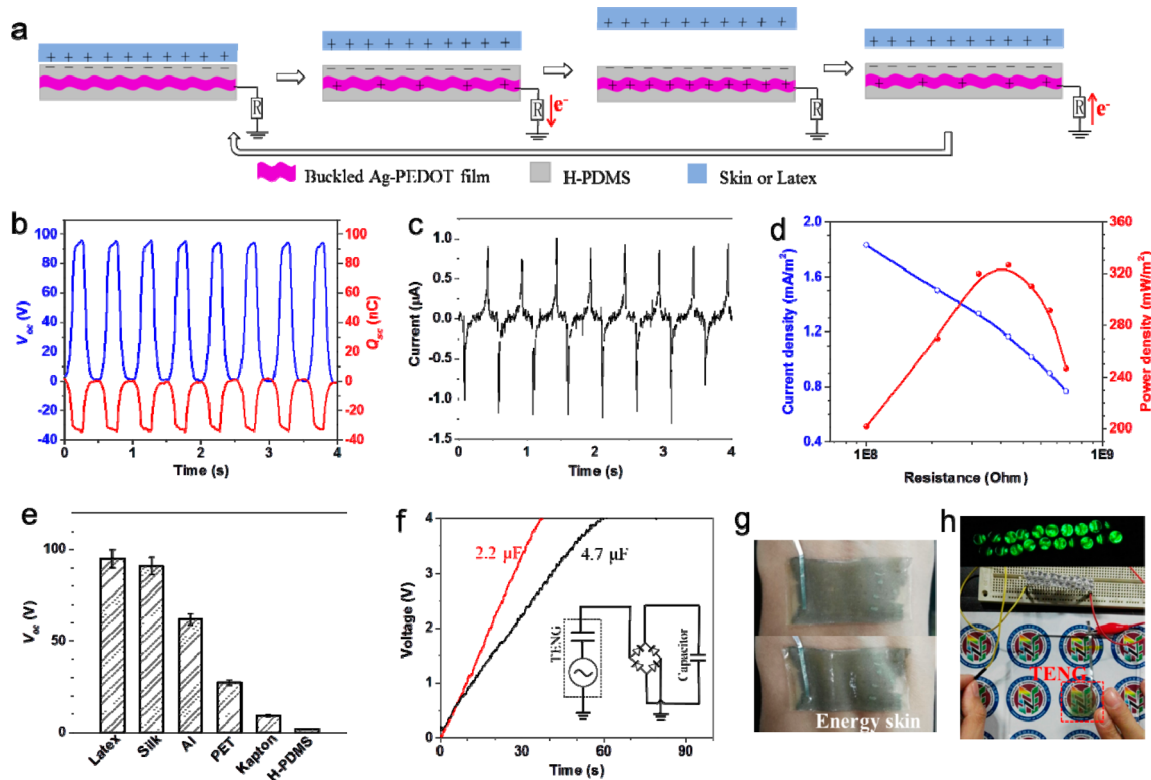


Figure 5. Characteristic electricity generation and human motion-energy harvesting by the soft TENG. (a) Working mechanism of the single-electrode TENG. (b) Output V_{oc} and Q_{sc} (c) I_{sc} and (d) areal power density of the TENG with contact–separation motions with a latex film. (e) V_{oc} of the TENG with relative motions of different materials. (f) Capacitor charging profiles of the TENG tapped by a human hand. The inset is a charging circuit. (g) Photos of a skin-like soft TENG deforming conformally on a wrist. (h) Photos of LEDs directly driven by tapping a TENG. The logo photos in (h) are used with permission from Beijing Institute of Nanoenergy and Nanosystems.

Ag-PEDOT film without prestrain, the resistance increases dramatically upon stretching, suggesting accumulated damages in the Ag-PEDOT film (Figure 3c). At a strain of about $\sim 17\%$, the resistance becomes infinity due to the fracture of the Ag-PEDOT film. In contrast, the wavy conductors show an almost stable resistance when the applied strain is smaller than the prestrain, in which only a slight increase in the resistance was observed (less than 50% increment). These findings are in accordance with previous buckled conductors.⁴⁸

In order to fabricate the single-electrode TENG, another H-PDMS layer was placed on top of the wavy Ag-PEDOT film. Given enough time (~ 12 h), the H-PDMS can fuse into the interstices between the buckled fringes and the sandwiched stacks bind tightly, as confirmed by a cross-sectional image (Figure S3a). But, it should be noted that the wavy structures are not damaged by this process and can still be observed by an optical microscope (Figure S3b,c). Therefore, a sandwiched wavy Ag-PEDOT film ($\sim 100\%$ prestrain) still showed stable resistance within the prestrain range (Figure 3c).

The H-PDMS is highly transparent (Figure 3d (i)). A 200 μm thick H-PDMS shows a transmittance of about $\sim 96\%$ in the range of visible light (Figure 3e). With a smooth Ag-PEDOT conductor transferred on top, the transmittance drops to $\sim 90\%$. For the wavy H-PDMS/Ag-PEDOT films with 50% and 100% prestrain, the transmittances decrease largely to $\sim 77\%$ and $\sim 70\%$, respectively, due to the increased light reflected by the rough surfaces. After placing a top layer of H-PDMS, the transmittances of the two samples further drop to $\sim 73\%$ and $\sim 67\%$, respectively. The optical images of all these samples are shown accordingly in Figure 3f. Interestingly, the

underneath letters cannot be distinguished for the wavy H-PDMS/Ag-PEDOT films with 100% prestrain, whereas, with an extra top H-PDMS layer, letters can be observed for the sandwiched film. This phenomenon is due to the diffuse reflection of rough surfaces.⁴⁹ After filling the fringe gaps by the top smooth H-PDMS, the underneath letters can be better resolved. Considering the trade-off between the stretchability and transparency, the soft TENG was fabricated with $\sim 50\%$ prestrain, as shown by Figure 3d (ii).

The composite H-PDMS/Ag-PEDOT film shows higher strength but worse elasticity than the bare H-PDMS (Figure S4), because the Ag-PEDOT film is stronger but more brittle compared to the elastomer substrate. An autonomous healing capability was still observed for the composite film, achieving a mechanical healing efficiency of about 86% (calculated based on fracture strain) at ambient conditions for 12 h after cutting by a razor blade (Figure 4a). Furthermore, the composite films are also electrically self-healable. To examine the electrical healing properties, we repeatedly cut the samples (about 4 mm \times 15 mm strips, original resistances are all around 100 Ω) thoroughly multiple times, and resistances were measured before and after 12 h of ambient healing each time. For each cutting, the cutting location is not the same but about ~ 3 mm away from the previous cutting site. The resistance of an H-PDMS/Ag-PEDOT film without prestrain was in the range 10–100 M Ω after cutting and recovered to ~ 3.8 times its initial value after 12 h of autonomous healing (Figure 4b). But, after the second cutting and healing, the electrical resistance was not recovered. As for the composite film and sandwiched film (with a top H-PDMS layer) with prestrain, stable electrical healing

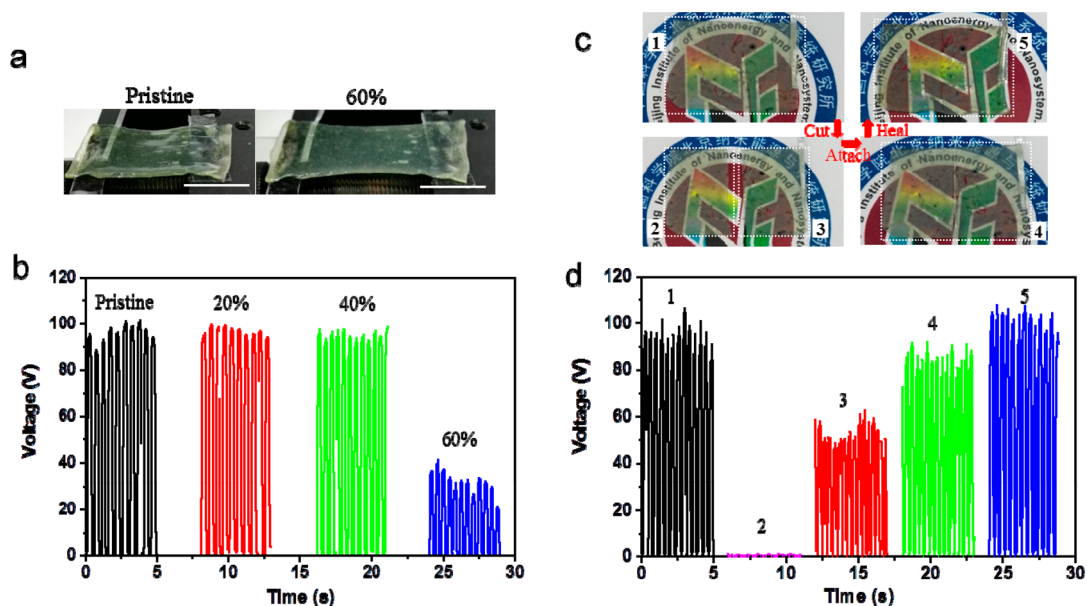


Figure 6. Stretchability and device healing properties of the soft TENG. (a) Photos of a TENG at pristine and 60% stretched states. (b) Output V_{oc} of the TENG after being stretched for different amounts of strain. (c) Photos and (d) V_{oc} of a soft TENG at pristine, cut, attached, and healed states. The labeling numbers in (d) are in accordance with the films in (c). Scale bar: 1 cm (a). The logo photos in (c) are used with permission from Beijing Institute of Nanoenergy and Nanosystems.

properties were observed even after cutting three times. For each cutting/healing, the resistance increment ratio ($\Delta R/R_0$) is in the range of about 60–170%, which is comparable with several previous reports.^{47,50,51}

Although the Ag-PEDOT film is not intrinsically healable, the healing process of the polymer substrate involves the fusing of H-PDMS back to repair the wound, which imparts a dragging force to the Ag-PEDOT film to bring them back into electrical contact, as schematically illustrated in Figure 4c and d. For the composite film without prestrain, a number of small cracks can be observed around the cutting area (Figure 4c (i)). After the healing, both small cracks and cutting cleft are healed (Figure 4c (ii)). Even under higher magnification by SEM, cracks are not noticeable (Figure 4c (iii)), and the recovered contact of Ag NWs can be observed (Figure 4c (iv)). As for the composite film with prestrain, no small crack is observed around the cutting area (Figure 4d (i)). After healing, the wound was cured, and the buckled Ag-PEDOT films at the two sides of the initial cleft are clearly observed to be back in contact (Figure 4d (ii–iv)). But, a tiny unhealed site is also observed (Figure 4d (ii)), which explains the increment in the resistance after the healing process. Since the buckled Ag-PEDOT film has better stretchability/flexibility, the cutting process cannot initiate damages to the film. This also explains why the composite or sandwiched films with prestrain have more stable multiple healing properties than that without prestrain.

With the above optimizations, the single-electrode soft TENG, which is stretchable, transparent, and both mechanically and electrically self-healable, has been successfully fabricated. The wavy Ag-PEDOT film is connected to the ground or reference electrode through an external load (Figure 5a). The contact of the top H-PDMS with an alien surface (materials different from H-PDMS) can naturally cause the electrification at the interface, generating electrostatic charges with opposite signs at the two surfaces. When the alien surface is moving away, a potential will be built up between the Ag-PEDOT and

the reference/grounding electrode at open-circuit conditions, due to the accumulated static charges in the H-PDMS. When the external load is connected, positive charges will be induced in the Ag-PEDOT electrode to screen the static charges and electrons flow from the Ag-PEDOT to the reference/grounding electrode. If the alien surface moves back, the electrons will flow in the opposite direction. By repeating the relative contact–separation motions, an alternative current will be generated. As discussed in Figure S5 and Note 1, the open-circuit voltage (V_{oc}) and transferred short-circuit charge quantity (Q_{sc}) are both 0 when two surfaces are in contact. When the two surfaces are far away, V_{oc} and Q_{sc} reach the maximum value and can be given as⁵²

$$V_{oc} = \frac{-\sigma A}{2C_0} \quad (1)$$

$$Q_{sc} = \frac{-\sigma A}{2} \quad (2)$$

where σ is the electrostatic charge density in H-PDMS, A is the contact interface area, and C_0 is the capacitance of the TENG.

To examine the output characteristics of the TENG, a commercial latex film was employed to have contact–separation motion with a TENG ($2 \times 3 \text{ cm}^2$ area). The frequency and speed of the motion were controlled by a stepping motor to be about 2 Hz and 0.2 m/s, respectively. The quantity of V_{oc} and Q_{sc} reached a maximum of about 94 V and 34 nC, respectively, when the two contacting surfaces are far away (Figure 5b). The peak short-circuit alternative current was measured to be about $1 \mu\text{A}$ (Figure 5c). By varying the resistance of the external loading, the maximum output areal power density was measured to be 327 mW/m^2 at a matched resistance of $400 \text{ M}\Omega$ (Figure 5d).

In practical applications, the soft TENG can have relative motions with many different materials as long as they are far from the H-PDMS in the tribo-negativity table.⁵³ The larger the difference they have in the tribo-series, the higher the amount of electrified static charges generated at the contacting

interfaces, and therefore the higher the measured peak value of V_{oc} . The peak values of V_{oc} when using commercial silk, Al, polyester (PET), and Kapton films as the alien contacting surfaces are 91, 62, 27, and 9 V, respectively, consistent with the established tribo-series table.⁵³ When two H-PDMS films are in contact–separation motion, almost no electrical signal is output, since their abilities in losing/gaining electrons are about the same. The TENG can also generate electricity when being touched by human skin. The peak values of the open-circuit voltage (Figure S6a) and short-circuit current (Figure S6b) were measured to be ~ 105 V and ~ 3 μ A when tapping the TENG with a human palm, respectively. The materials' universality of triboelectrification effect is important for the single-electrode TENG, which ensures electricity generation for different applications.

The applicability of the TENG as a soft energy skin to harvest human motion energies was demonstrated (Figure 5f). A TENG skin was attached on a wrist, which can accommodate itself to the deformation of the wrist and remain attached conformally (Figure 5g). By tapping the TENG with the other hand, the rectified electricity (Figure S6c) can charge commercial capacitors of 2.2 and 4.7 μ F to 4 V in 35 and 58 s, respectively. The charging rate is 250 and 320 nC/s when charging a 2.2 and 4.7 μ F capacitor, respectively. The equivalent rectifying circuit is shown in the inset in Figure 5g. With this circuit, the pulsed alternative current can be converted into direct current and stored in capacitors for a stable power supply of small electronics.^{54,55} Meantime, the electricity generated by the TENG can directly light up 20 green light-emitting diodes (LEDs) connected in series, as shown in Figure 5h and Supplementary Movie 1.

The stretchability of the TENG was further examined. As discussed above, the ultimate stretchability of the buckled Ag-PEDOT electrode was determined by the prestrain of the H-PDMS. Our TENG was fabricated with 50% prestrained H-PDMS, in order to balance the stretchability and transparency. The output V_{oc} of a soft TENG film was measured after being stretched uniaxially for 10 cycles by a linear motor (Figure 6a). Compared with the pristine TENG, the V_{oc} shows no noticeable difference after being stretched to 20% and 40%, but a significant decrease of the V_{oc} was observed after being stretched to 60% (Figure 6b). By stretching the TENG beyond the prestrain, cracks and damage will quickly initiate in the Ag-PEDOT electrode, resulting in the loss of electrical contact of the Ag-PEDOT film. Therefore, the induced charges in the electrode and the output electrical signals will decrease dramatically. However, the TENG can work appropriately when the applied strain is lower than the prestrain.

To evaluate the self-healing ability, a soft TENG was cut in the middle by a razor blade, attached back, and then healed at ambient conditions for 12 h, as shown in Figure 6c. The pristine complete TENG film (film 1) can output V_{oc} with a peak value of about ~ 100 V (Figure 6d). After being cut into two pieces, film 2 without electrical connection shows no electrical signal, while the other half-piece (film 3) with electrical connection still outputs a V_{oc} of about half of the pristine value, because that the contacting area and therefore the electrostatic charges of the H-PDMS are about half (eq 2). After attaching the two pieces back, the output of TENG film 4 increases immediately close to the pristine value. According to our measurement, the attached film 4 shows a resistance in the range of 10–100 M Ω across the cleft. But, as demonstrated by Figure 5d, the internal resistance of the TENG is about 400

M Ω , so the electrical output can be largely recovered despite the increase in the electrode resistance. After the autonomous healing for 12 h, the electrical generation by the healed TENG film 5 can be almost 100% recovered, suggesting the recovery of both the Ag-PEDOT electrode and the dielectric H-PDMS layers. This self-healing ability of the TENG device was also demonstrated by Supplementary Movie 2.

CONCLUSIONS

Soft transparent conductors, which can withstand certain degrees of deformation and can recover from damage spontaneously, are essential for many electronic and energy devices.¹³ This work presents a methodology for fabricating a self-healable, stretchable, and transparent electrical conductor. Self-healable polymers are of vital importance for developing various healable materials and devices. Our healable PDMS elastomer, based on reversible imine bonds, achieved a high healing efficiency (94%) at ambient conditions without external stimuli. From our above results, it was found that the trade-off between the stretchability and transparency should be considered for the design of soft transparent conductors, while the flexibility/stretchability is beneficial for reliable healing ability, since less mechanical damage is initiated upon mechanical stimuli. The top sealing H-PDMS layer was found to be able to not only protect the buckled Ag-PEDOT film but also avoid the diffuse reflection by the wavy film.

This work also suggests a feasible approach for soft power sources. Despite the rapid advancements in next-generation soft electronics, compatible energy devices will be the next challenge for their progress and viable applications. With the required high flexibility/stretchability, transparency, and healing ability, the choice of energy-conversion strategy is rare. Our TENG achieves $\sim 100\%$ healing efficiency, $\sim 50\%$ stretchability, and $\sim 73\%$ transmittance. The stretchability and transmittance can further be tuned by the prestrain of the H-PDMS substrate. The high output of our TENG-based energy skin, especially the high voltage (~ 100 V), makes it highly promising for powering many soft devices.

METHODS

Fabrication of the Healable Elastomer. Healable PDMS was synthesized by mixing 2 g of bis(amine)-terminated poly(dimethylsiloxane) ($M_n = 5000\text{--}7000$ g mol⁻¹, Gelest DMS-A21) and a 1 mL solution of 0.4 M 1,3,5-triformylbenzene (Ark Pharm, Inc.) in dimethylformamide (DMF). The mixture was dried in a polyvinylidene fluoride (PVDF) container at room temperature for 12 h and then heated to 80 °C for 5 h. Imine bonds were formed, and the PDMS chains were linked to generate the transparent and healable elastomer.⁴⁴

Fabrication of the Buckled Ag-PEDOT Electrode and Soft TENG. The Ag NW film was prepared by spray coating a 2 mg/mL solution of Ag NWs (Nanjing XFNANO Materials Tech Co., Ltd.) in 2-propanol onto a heated (~ 50 °C) PVDF substrate. The PEDOT solution (Clevios PH1000) was first treated with 8 wt % dimethyl sulfoxide (DMSO) in air at ~ 80 °C for 1 h for better conductivity. Then, the treated PEDOT was spin coated on the Ag NW film at a rotating speed of 2000 rpm for 30 s. The Ag-PEDOT film was obtained by drying at 100 °C in air for 1 h.

The buckled Ag-PEDOT film was prepared through a prestrain–release–buckling process. The H-PDMS was first stretched uniaxially to certain degrees of strain and was then attached onto the Ag-PEDOT film. Then, the Ag-PEDOT film was transferred onto the surface of strained H-PDMS when detaching it from the substrate. By releasing the stress applied on the H-PDMS, the Ag-PEDOT film will naturally form a buckled morphology. The soft TENG was then

fabricated by sealing the buckled Ag-PEDOT electrode with an extra top layer of H-PDMS. Given enough time, the interstices between the buckling fringes can be filled by the top H-PDMS.

Measurements and Characterizations. The mechanical tensile tests were conducted by an ESM301/Mark-10 system. The gauge dimensions of tested samples are about 10 mm × 4 mm × 0.4 mm. For the tensile test, the train rate was fixed at 40 mm/min. For mechanical healing tests, the samples were cut completely by a commercial razor blade, followed by healing at ambient conditions for different periods of time. After cutting the samples, the cut two pieces were always not moved before the measurements of mechanical and electrical properties. Otherwise, the two cut Ag-PEDOT films may not contact accurately after healing. The resistances were measured by a two-probe method. For the measurement of electricity generation, a step motor (Linmot E1100) was used to provide the input of mechanical motions. For all the tests of energy generation by the TENG, the speed (0.2 m/s) and frequency (~2 Hz) of the step motor were fixed. The voltage and charge quantity were recorded by a Keithley electrometer 6514, and the current was recorded with a Stanford low-noise preamplifier SR570.

The UV-vis spectra were obtained by a Shimadzu UV-3600 spectrometer. FTIR spectra were taken by a Bruker/VERTEX80v. The SEM images were taken with a Hitachi SU8200, and the optical microscopy images were taken by an Axio Imager.M2m.

ASSOCIATED CONTENT

Supporting Information

The Supporting Information is available free of charge on the ACS Publications website at DOI: 10.1021/acsnano.8b02479.

FTIR of the H-PDMS and commercial Sylard 184; SEM images of Ag NW film, Ag-PEDOT composite film before and after transferred to H-PDMS, and cross-sectional SEM image of soft TENG; optical microscopy of buckled Ag-PEDOT film without and with top H-PDMS layer; comparison of the tensile tests of bare H-PDMS and H-PDMS/Ag-PEDOT; equivalent circuit and calculation of the output V_{oc}/Q_{sc} of TENG at single-electrode mode; output characteristics of the TENG by contact-separation motion with human skin. (PDF)

Movie 1: electricity generated by the TENG directly lighting up 20 green LEDs connected in series (AVI)

Movie 2: self-healing ability of the TENG device (AVI)

AUTHOR INFORMATION

Corresponding Authors

*E-mail: puxiong@binn.cas.cn.

*E-mail: huweigu@binn.cas.cn.

*E-mail: zlwang@gatech.edu.

ORCID

Xiong Pu: 0000-0002-1254-8503

Junyi Zhai: 0000-0001-8900-4638

Weiguo Hu: 0000-0002-8614-0359

Zhong Lin Wang: 0000-0002-5530-0380

Notes

The authors declare no competing financial interest.

ACKNOWLEDGMENTS

The authors are grateful for the support from National Key Research and Development Program of China (2016YFA0202703), National Natural Science Foundation of China (Grant Nos. 51603013, 61574018, and 51432005), the “Thousands Talents” Program for pioneer researcher and his innovation team, China, the Youth Innovation Promotion

Association of CAS, and the “Hundred Talents Program” of CAS.

REFERENCES

- (1) Rogers, J. A.; Huang, Y. G. A Curvy, Stretchy Future for Electronics. *Proc. Natl. Acad. Sci. U. S. A.* **2009**, *106*, 10875–10876.
- (2) Kim, D.-H.; Lu, N.; Ma, R.; Kim, Y.-S.; Kim, R.-H.; Wang, S.; Wu, J.; Won, S. M.; Tao, H.; Islam, A.; Yu, K. J.; Kim, T.-i.; Chowdhury, R.; Ying, M.; Xu, L.; Li, M.; Chung, H.-J.; Keum, H.; McCormick, M.; Liu, P.; et al. Epidermal Electronics. *Science* **2011**, *333*, 838–843.
- (3) Chortos, A.; Liu, J.; Bao, Z. Pursuing Prosthetic Electronic Skin. *Nat. Mater.* **2016**, *15*, 937–950.
- (4) Liu, T.; Liu, M.; Dou, S.; Sun, J.; Cong, Z.; Jiang, C.; Du, C.; Pu, X.; Hu, W.; Wang, Z. L. Triboelectric-Nanogenerator-Based Soft Energy-Harvesting Skin Enabled by Toughly Bonded Elastomer/Hydrogel Hybrids. *ACS Nano* **2018**, *12*, 2818–2826.
- (5) Park, J.; Kim, M.; Lee, Y.; Lee, H. S.; Ko, H. Fingertip Skin-Inspired Microstructured Ferroelectric Skins Discriminate Static/Dynamic Pressure and Temperature Stimuli. *Sci. Adv.* **2015**, *1*, e1500661.
- (6) Lee, H.; Song, C.; Hong, Y. S.; Kim, M. S.; Cho, H. R.; Kang, T.; Shin, K.; Choi, S. H.; Hyeon, T.; Kim, D.-H. Wearable/Disposable Sweat-Based Glucose Monitoring Device with Multistage Transdermal Drug Delivery Module. *Sci. Adv.* **2017**, *3*, e1601314.
- (7) Son, D.; Lee, J.; Qiao, S.; Ghaffari, R.; Kim, J.; Lee, J. E.; Song, C.; Kim, S. J.; Lee, D. J.; Jun, S. W.; Yang, S.; Park, M.; Shin, J.; Do, K.; Lee, M.; Kang, K.; Hwang, C. S.; Lu, N.; Hyeon, T.; Kim, D.-H. Multifunctional Wearable Devices for Diagnosis and Therapy of Movement Disorders. *Nat. Nanotechnol.* **2014**, *9*, 397–404.
- (8) Rogers, J. A.; Someya, T.; Huang, Y. Materials and Mechanics for Stretchable Electronics. *Science* **2010**, *327*, 1603–1607.
- (9) Benight, S. J.; Wang, C.; Tok, J. B. H.; Bao, Z. Stretchable and Self-Healing Polymers and Devices for Electronic Skin. *Prog. Polym. Sci.* **2013**, *38*, 1961–1977.
- (10) Schroeder, T. B. H.; Guha, A.; Lamoureux, A.; VanRenterghem, G.; Sept, D.; Shtein, M.; Yang, J.; Mayer, M. An Electric-Eel-Inspired Soft Power Source from Stacked Hydrogels. *Nature* **2017**, *552*, 214–218.
- (11) Han, F.; Meng, G.; Zhou, F.; Song, L.; Li, X.; Hu, X.; Zhu, X.; Wu, B.; Wei, B. Dielectric Capacitors with Three-Dimensional Nanoscale Interdigital Electrodes for Energy Storage. *Sci. Adv.* **2015**, *1*, e1500605.
- (12) Chen, D.; Wang, D.; Yang, Y.; Huang, Q.; Zhu, S.; Zheng, Z. Self-Healing Materials for Next-Generation Energy Harvesting and Storage Devices. *Adv. Energy Mater.* **2017**, *7*, 1700890.
- (13) Luo, C. S.; Wan, P.; Yang, H.; Shah, S. A. A.; Chen, X. Healable Transparent Electronic Devices. *Adv. Funct. Mater.* **2017**, *27*, 1606339.
- (14) Fan, F.-R.; Tian, Z.-Q.; Wang, Z. L. Flexible triboelectric generator. *Nano Energy* **2012**, *1* (2), 328–334.
- (15) Wang, Z. L. On Maxwell's Displacement Current for Energy and Sensors: the Origin of Nanogenerators. *Mater. Today* **2017**, *20*, 74–82.
- (16) Wang, Z. L.; Chen, J.; Lin, L. Progress in Triboelectric Nanogenerators as A New Energy Technology and Self-Powered Sensors. *Energy Environ. Sci.* **2015**, *8*, 2250–2282.
- (17) Pu, X.; Hu, W.; Wang, Z. L. Toward Wearable Self-Charging Power Systems: the Integration of Energy-Harvesting and Storage Devices. *Small* **2018**, *14*, 1702817.
- (18) Li, J.; Wang, X. Research Update: Materials Design of Implantable Nanogenerators for Biomechanical Energy Harvesting. *APL Mater.* **2017**, *5*, 073801.
- (19) Khan, U.; Kim, T.-H.; Lee, K. H.; Lee, J.-H.; Yoon, H.-J.; Bhatia, R.; Sameera, I.; Seung, W.; Ryu, H.; Falconi, C.; Kim, S.-W. Self-Powered Transparent Flexible Graphene Microheaters. *Nano Energy* **2015**, *17*, 356–365.
- (20) Yu, Y.; Wang, X. Chemical Modification of Polymer Surfaces for Advanced Triboelectric Nanogenerator Development. *Extreme Mechanics Letters* **2016**, *9*, 514–530.

- (21) Qian, Z.; Qijie, L.; Qingliang, L.; Fang, Y.; Xin, Z.; Mingyuan, M.; Fangfang, G.; Yue, Z. Service Behavior of Multifunctional Triboelectric Nanogenerators. *Adv. Mater.* **2017**, *29*, 1606703.
- (22) Qijie, L.; Qian, Z.; Xiaoqin, Y.; Xinqin, L.; Linhong, H.; Fang, Y.; Mingyuan, M.; Yue, Z. Recyclable and Green Triboelectric Nanogenerator. *Adv. Mater.* **2017**, *29*, 1604961.
- (23) Qian, Z.; Qijie, L.; Zheng, Z.; Zhuo, K.; Qingliang, L.; Yi, D.; Mingyuan, M.; Fangfang, G.; Xuan, Z.; Yue, Z. Electromagnetic Shielding Hybrid Nanogenerator for Health Monitoring and Protection. *Adv. Funct. Mater.* **2018**, *28*, 1703801.
- (24) Yu, A.; Pu, X.; Wen, R.; Liu, M.; Zhou, T.; Zhang, K.; Zhang, Y.; Zhai, J.; Hu, W.; Wang, Z. L. Core-Shell-Yarn-Based Triboelectric Nanogenerator Textiles as Power Cloths. *ACS Nano* **2017**, *11*, 12764–12771.
- (25) Pu, X.; Li, L.; Liu, M.; Jiang, C.; Du, C.; Zhao, Z.; Hu, W.; Wang, Z. L. Wearable Self-Charging Power Textile Based on Flexible Yarn Supercapacitors and Fabric Nanogenerators. *Adv. Mater.* **2016**, *28*, 98–105.
- (26) Kim, S.; Gupta, M. K.; Lee, K. Y.; Sohn, A.; Kim, T. Y.; Shin, K. S.; Kim, D.; Kim, S. K.; Lee, K. H.; Shin, H. J.; Kim, D. W.; Kim, S. W. Transparent Flexible Graphene Triboelectric Nanogenerators. *Adv. Mater.* **2014**, *26*, 3918–3925.
- (27) Liang, Q.; Yan, X.; Gu, Y.; Zhang, K.; Liang, M.; Lu, S.; Zheng, X.; Zhang, Y. Highly Transparent Triboelectric Nanogenerator for Harvesting Water-Related Energy Reinforced by Antireflection Coating. *Sci. Rep.* **2015**, *5*, 9080.
- (28) Liang, Q.; Yan, X.; Liao, X.; Zhang, Y. Integrated Multi-Unit Transparent Triboelectric Nanogenerator Harvesting Rain Power for Driving Electronics. *Nano Energy* **2016**, *25*, 18–25.
- (29) Lai, Y.-C.; Deng, J.; Niu, S.; Peng, W.; Wu, C.; Liu, R.; Wen, Z.; Wang, Z. L. Electric Eel-Skin-Inspired Mechanically Durable and Super-Stretchable Nanogenerator for Deformable Power Source and Fully Autonomous Conformable Electronic-Skin Applications. *Adv. Mater.* **2016**, *28*, 10024–10032.
- (30) Yi, F.; Wang, X.; Niu, S.; Li, S.; Yin, Y.; Dai, K.; Zhang, G.; Lin, L.; Wen, Z.; Guo, H. A Highly Shape-Adaptive, Stretchable Design Based on Conductive Liquid for Energy Harvesting and Self-Powered Biomechanical Monitoring. *Sci. Adv.* **2016**, *2*, e1501624.
- (31) Pu, X.; Liu, M.; Chen, X.; Sun, J.; Du, C.; Zhang, Y.; Zhai, J.; Hu, W.; Wang, Z. L. Ultrastretchable, Transparent Triboelectric Nanogenerator as Electronic Skin for Biomechanical Energy Harvesting and Tactile Sensing. *Sci. Adv.* **2017**, *3*, e1700015.
- (32) Zhang, Y.; Yang, Y.; Gu, Y.; Yan, X.; Liao, Q.; Li, P.; Zhang, Z.; Wang, Z. Performance and Service Behavior in 1-D Nanostructured Energy Conversion Devices. *Nano Energy* **2015**, *14*, 30–48.
- (33) Huynh, T.-P.; Sonar, P.; Haick, H. Advanced Materials for Use in Soft Self-Healing Devices. *Adv. Mater.* **2017**, *29*, 1604973.
- (34) Lee, J. H.; Hinchet, R.; Kim, S. K.; Kim, S.; Kim, S.-W. Shape Memory Polymer-Based Self-Healing Triboelectric Nanogenerator. *Energy Environ. Sci.* **2015**, *8*, 3605–3613.
- (35) Parida, K.; Kumar, V.; Jiangxin, W.; Bhavanasi, V.; Bendi, R.; Lee, P. S. Highly Transparent, Stretchable, and Self-Healing Ionic-Skin Triboelectric Nanogenerators for Energy Harvesting and Touch Applications. *Adv. Mater.* **2017**, *29*, 1702181.
- (36) Xu, W.; Huang, L.-B.; Hao, J. Fully Self-healing and Shape-tailorable Triboelectric Nanogenerators Based on Healable Polymer and Magnetic-assisted Electrode. *Nano Energy* **2017**, *40*, 399–407.
- (37) Deng, J.; Kuang, X.; Liu, R.; Ding, W.; Wang, A. C.; Lai, Y.-C.; Dong, K.; Wen, Z.; Wang, Y.; Wang, L.; Qi, H. J.; Zhang, T.; Wang, Z. L. Vitrimers Elastomer-Based Jigsaw Puzzle-Like Healable Triboelectric Nanogenerator for Self-Powered Wearable Electronics. *Adv. Mater.* **2018**, *30*, 1705918.
- (38) Blaiszik, B. J.; Kramer, S. L. B.; Grady, M. E.; McIlroy, D. A.; Moore, J. S.; Sottos, N. R.; White, S. R. Autonomic Restoration of Electrical Conductivity. *Adv. Mater.* **2012**, *24*, 398–401.
- (39) Tee, B. C. K.; Wang, C.; Allen, R.; Bao, Z. An Electrically and Mechanically Self-Healing Composite with Pressure- and Flexion-Sensitive Properties for Electronic Skin Applications. *Nat. Nanotechnol.* **2012**, *7*, 825–832.
- (40) Li, C.-H.; Wang, C.; Keplinger, C.; Zuo, J.-L.; Jin, L.; Sun, Y.; Zheng, P.; Cao, Y.; Lissel, F.; Linder, C.; You, X.-Z.; Bao, Z. A Highly Stretchable Autonomous Self-Healing Elastomer. *Nat. Chem.* **2016**, *8*, 618–624.
- (41) Chen, X.; Dam, M. A.; Ono, K.; Mal, A.; Shen, H.; Nutt, S. R.; Sheran, K.; Wudl, F. A Thermally Re-mendable Cross-Linked Polymeric Material. *Science* **2002**, *295*, 1698–1702.
- (42) Canadell, J.; Goossens, H.; Klumperman, B. Self-Healing Materials Based on Disulfide Links. *Macromolecules* **2011**, *44*, 2536–2541.
- (43) Taynton, P.; Ni, H.; Zhu, C.; Yu, K.; Loob, S.; Jin, Y.; Qi, H. J.; Zhang, W. Repairable Woven Carbon Fiber Composites with Full Recyclability Enabled by Malleable Polyimine Networks. *Adv. Mater.* **2016**, *28*, 2904–2909.
- (44) Zhang, B.; Zhang, P.; Zhang, H.; Yan, C.; Zheng, Z.; Wu, B.; Yu, Y. A Transparent, Highly Stretchable, Autonomous Self-Healing Poly(dimethyl siloxane) Elastomer. *Macromol. Rapid Commun.* **2017**, *38*, 1700110.
- (45) Kathan, M.; Kovaříček, P.; Jurissek, C.; Senf, A.; Dallmann, A.; Thünemann, A. F.; Hecht, S. Control of Imine Exchange Kinetics with Photoswitches to Modulate Self-Healing in Polysiloxane Networks by Light Illumination. *Angew. Chem., Int. Ed.* **2016**, *55*, 13882–13886.
- (46) Bowden, N.; Brittain, S.; Evans, A. G.; Hutchinson, J. W.; Whitesides, G. M. Spontaneous Formation of Ordered Structures in Thin Films of Metals Supported on An Elastomeric Polymer. *Nature* **1998**, *393*, 146–149.
- (47) Gong, C.; Liang, J.; Hu, W.; Niu, X.; Ma, S.; Hahn, H. T.; Pei, Q. A Healable, Semitransparent Silver Nanowire-Polymer Composite Conductor. *Adv. Mater.* **2013**, *25*, 4186–4191.
- (48) Yao, S.; Zhu, Y. Nanomaterial-Enabled Stretchable Conductors: Strategies, Materials and Devices. *Adv. Mater.* **2015**, *27*, 1480–1511.
- (49) Chen, X.; Pu, X.; Jiang, T.; Yu, A.; Xu, L.; Wang, Z. L. Tunable Optical Modulator by Coupling a Triboelectric Nanogenerator and a Dielectric Elastomer. *Adv. Funct. Mater.* **2017**, *27*, 1603788.
- (50) Li, Y.; Chen, S.; Wu, M.; Sun, J. Polyelectrolyte Multilayers Impart Healability to Highly Electrically Conductive Films. *Adv. Mater.* **2012**, *24*, 4578–4582.
- (51) Sun, H.; You, X.; Jiang, Y.; Guan, G.; Fang, X.; Deng, J.; Chen, P.; Luo, Y.; Peng, H. Self-Healable Electrically Conducting Wires for Wearable Microelectronics. *Angew. Chem., Int. Ed.* **2014**, *53*, 9526–9531.
- (52) Niu, S.; Wang, Z. L. Theoretical Systems of Triboelectric Nanogenerators. *Nano Energy* **2015**, *14*, 161–192.
- (53) Wang, Z. L. Triboelectric Nanogenerators as New Energy Technology for Self-Powered Systems and as Active Mechanical and Chemical Sensors. *ACS Nano* **2013**, *7*, 9533–9557.
- (54) Pu, X.; Li, L.; Song, H.; Du, C.; Zhao, Z.; Jiang, C.; Cao, G.; Hu, W.; Wang, Z. L. A Self-Charging Power Unit by Integration of a Textile Triboelectric Nanogenerator and a Flexible Lithium-Ion Battery for Wearable Electronics. *Adv. Mater.* **2015**, *27*, 2472–2478.
- (55) Wang, J.; Li, S.; Yi, F.; Zi, Y.; Lin, J.; Wang, X.; Xu, Y.; Wang, Z. L. Sustainably Powering Wearable Electronics Solely by Biomechanical Energy. *Nat. Commun.* **2016**, *7*, 12744.